

## Luminescence from colloidal 3C-SiC nanocrystals in different solvents

J. Y. Fan,<sup>a)</sup> X. L. Wu,<sup>a),b)</sup> H. X. Li, and H. W. Liu

National Laboratory of Solid State Microstructures & Department of Physics, Nanjing University, Nanjing 210093, People's Republic of China

G. G. Siu<sup>b)</sup> and Paul K. Chu<sup>b)</sup>

Department of Physics and Materials Science, City University of Hong Kong, Tat Chee Avenue, Kowloon, Hong Kong, People's Republic of China

(Received 26 July 2005; accepted 29 November 2005; published online 25 January 2006)

We have investigated the role of the solvents in the luminescence from colloidal 3C-SiC suspensions. By dispersing electrochemically etched polycrystalline 3C-SiC wafers in water, ethanol, or toluene, we have fabricated suspensions of 3C-SiC nanocrystals that exhibit intense photoluminescence. By taking into account the quantum confinement effect and observed size distributions of the 3C-SiC crystallites, a simple model is formulated to explain the photoluminescence spectra. Our results show that the colloidal 3C-SiC nanocrystals are robust and intense emitters that have good chemical stability and biocompatibility. They are thus useful in biotechnology and nano-optoelectronics applications. © 2006 American Institute of Physics. [DOI: 10.1063/1.2168018]

Recently, aqueous suspensions of 3C-SiC nanocrystals showing intense emissions have been successfully fabricated by dispersing electrochemically etched porous polycrystalline 3C-SiC wafers in water.<sup>1</sup> The photoluminescence (PL) spectrum exhibits continuous redshifts with increasing excitation wavelengths and provides clear evidence of quantum confinement.<sup>2,3</sup> This effect has been predicted theoretically<sup>4,5</sup> but never obviously observed in experiments<sup>6-14</sup> due to existing much more complicated surface states and reconstructions compared with that of silicon.<sup>15,16</sup> Based on this method, 3C-SiC/polystyrene composite films that luminescence in the blue region have been prepared.<sup>17</sup> However, it has been shown that the porous 3C-SiC layers before ultrasonic treatment do not luminesce,<sup>1,17</sup> and this property is quite different from that of Si.<sup>18</sup> Therefore, it is suspected that the solvent, water, may play a special role in the luminescence from the 3C-SiC solutions. In order to study the solvent effects and luminescence mechanism, we have investigated the luminescence of 3C-SiC suspensions in different solvents and report our results in this letter. By taking into account the size distributions of the crystallites, a simple model is proposed to explain the spectral behavior confirming that the emission arises from band edge recombination of the carriers in the 3C-SiC nanocrystals. We have also determined the necessary conditions in order for quantum confinement to take effect in the 3C-SiC crystallites.

The fabrication and characterization of 3C-SiC nanocrystals were all performed in air at room temperature. Three identical polycrystalline 3C-SiC wafers were anodically etched in HF ethanol (40 wt% HF : 98 wt% C<sub>2</sub>H<sub>5</sub>OH=2:1) at a current density 40 mA/cm<sup>2</sup> for 60 min while the samples were illuminated by a 150 W halogen lamp from above to further increase the porosities. The specimens were subsequently ultrasonically treated in water, ethanol, and toluene solvents with the same volume for 10 min, respec-

tively. During this process, the porous 3C-SiC layers on the wafers crumbled into nanometer-sized crystallites and dispersed uniformly in the respective solutions.<sup>1,18,19</sup> For convenience, the 3C-SiC nanocrystal suspensions in water, ethanol, and toluene are designated as samples W, E, and T, respectively.

Figure 1(a) shows the PL spectra taken on a FluoroMax-2 fluorescence spectrometer from samples W, E, and T. The emission spectra are very smooth showing no substructures and a typical full width at half maximum of 120 nm. In contrast, no emission was observed from the as-etched porous polycrystalline 3C-SiC wafer [Fig. 1(b)]. The PL spectra of all the samples exhibit monotonic redshifts with increasing excitation wavelengths, as shown in Fig.

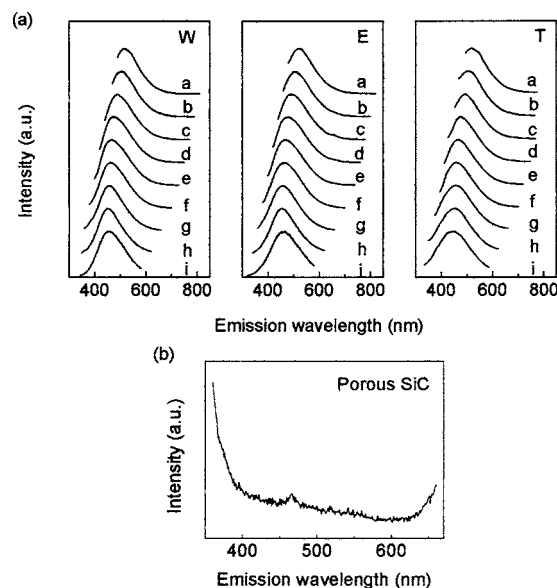


FIG. 1. (Color online) (a) a-i Normalized PL spectra recorded excited by the 460, 440, 420, 400, 380, 360, 340, 320, and 300 nm lines, respectively. W, E, and T refer to the water, ethanol, and toluene suspensions of the 3C-SiC nanocrystals, respectively. (b) PL spectrum from as-etched porous polycrystalline 3C-SiC.

<sup>a)</sup>Also affiliated with Department of Physics & Materials Science, City University of Hong Kong.

<sup>b)</sup>Authors to whom correspondence should be addressed; electronic mail: hkxluw@nju.edu.cn, appggsiu@cityu.edu.cn, paul.chu@cityu.edu.hk

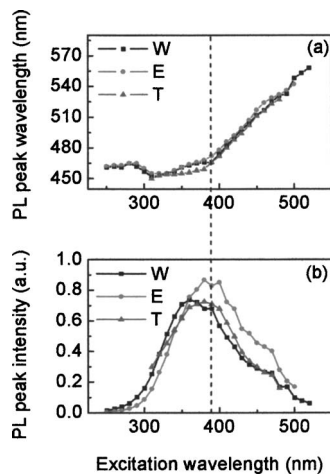


FIG. 2. (Color online) PL peak wavelength (a) and intensity (b) as a function of the excitation wavelength for samples W, E, and T.

2(a). Figure 2(b) displays the PL peak intensities as a function of the excitation wavelengths from 250 to 520 nm. The maximum intensity is observed at an excitation wavelength of  $\sim 385$  nm.

To investigate the mechanism, transmission electron microscopy (TEM) was performed using a TECNAL\_F20 TEM at 200 kV. Figure 3(a) depicts a high-resolution TEM image of two typical 3C-SiC particles. They are nearly spherical and highly crystalline, with lattice fringes spaced 2.55 Å apart that are close to the value of the (111) plane of bulk 3C-SiC (2.52 Å).<sup>20</sup> The histograms of the diameters measured from over 220 3C-SiC crystallites for each sample are displayed in Fig. 3(b). A Gaussian fit yields the mean diameters (or most probable diameters) of 3.87, 3.94, or 3.72 nm for samples W, E, and T, respectively. Since the three suspensions have been prepared under the same conditions, the crystallites should have similar size distributions as shown in Fig. 3(b). In fact, under a specific excitation, the emission spectra of these samples have similar shapes [Fig. 1(a)], almost equal values of peak wavelengths [Fig. 2(a)], and small intensity contrasts [Fig. 2(b)]. These observations suggest that the luminescence originates from the intrinsic band edge

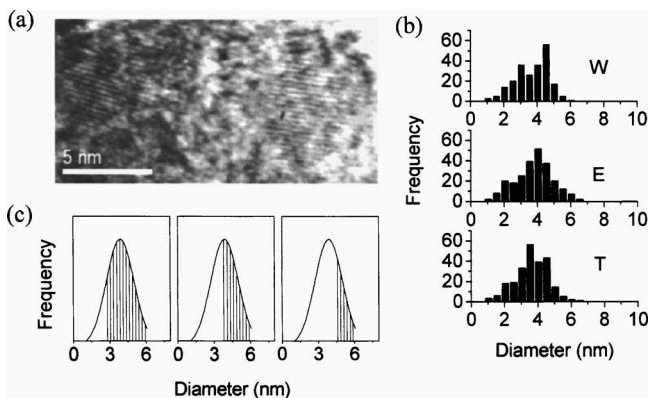


FIG. 3. (Color online) (a) High-resolution TEM image of two typical 3C-SiC particles with diameters of 3.6 and 6.6 nm, respectively. (b) Size histograms showing the average dimension calculated from over 220 particles from each sample. (c) Schematic diagrams showing the size range of 3C-SiC crystallites that can be excited under excitations, from left to right corresponding to excitation wavelengths shorter than, equal to, and longer than  $\sim 385$  nm, respectively. The shaded area represents the size range of the excitable particles.

recombination of the carriers in the 3C-SiC crystallites. The small contrast in the emission intensities may be ascribed to different barrier heights of the carriers confined in the 3C-SiC particles caused by the different liquid media.<sup>3</sup>

The PL spectral characteristics can be interpreted by considering quantum confinement and the size distributions of the particles. Each sample contains 3C-SiC crystallites with different sizes, thereby leading to wide emission spectra [Fig. 1(a)]. Smaller particles have higher absorption edges,<sup>21</sup> and so the carriers in more and more small 3C-SiC crystallites cannot be excited as the excitation is shifted to a lower energy. Consequently, a continuous redshift is observed in the PL spectrum [Fig. 2(a)]. Based on the PL and TEM results, it is postulated that the excitation at the turning point of the two distinct regions shown in Fig. 2(a) ( $\sim 385$  nm) simply corresponds to the absorption edge of the 3C-SiC particles with the mean size. This situation is schematically shown in the middle diagram in Fig. 3(c) in which the Gaussian fit of the size distribution of the particles in sample W is plotted. The shaded area represents the size range of particles that can be excited by a wavelength of  $\sim 385$  nm. The left and right diagrams correspond to the cases of higher and lower excitation energies, respectively. At a higher excitation energy, the carriers in the 3C-SiC crystallites with most probable size can always be excited, and so the PL only exhibits slight redshifts at excitations from 250 to  $\sim 385$  nm [Fig. 2(a)]. On the other hand, at a lower excitation energy (wavelength  $> \sim 385$  nm), the size of the smallest excitable particles increases quickly with increasing excitation wavelength, as shown in the right diagram in Fig. 3(c). As a result, the PL band quickly shifts to red in this region [Fig. 2(a)] until reaching  $\sim 560$  nm at excitation of  $\sim 520$  nm, which is close to the band gap of bulk 3C-SiC at  $T=300$  K.<sup>22</sup> Thus, no emission can be observed at excitation wavelengths beyond  $\sim 520$  nm and it is in agreement with the empirical results.

The variations of the emission intensity with excitation wavelengths [Fig. 2(b)] provide further evidence to support our model. As the excitation wavelength is increased from 250 to  $\sim 385$  nm, the 3C-SiC particles with the mean or most probable size can always be excited and the emission intensity always increases. From  $\sim 385$  nm on, the size of the smallest excitable particles increases and the number of luminescent particles decreases quickly. As a result, the emission intensity drops quickly and to zero at an excitation wavelength of 520 nm. Hence, the PL peak intensity exhibits a maximum at around 385 nm, in accordance with Fig. 2(b).

Figure 4 shows the measured and calculated values of the optical gaps of 3C-SiC crystallites with different diameters. The experimental values are obtained from the 3C-SiC crystallites with the mean or most probable sizes in the three samples. Their optical gaps correspond to the emission wavelengths at the respective turning points. The theoretical values are the optical gaps of 3C-SiC quantum dots calculated by the effective mass approximation method.<sup>4</sup> The experimental and theoretical results agree well within our margin of error. The resonant Stokes shifts are further calculated from the crystallites with the mean size to be 0.52, 0.55, and 0.57 eV for samples W, E, and T, respectively. They are contrast values between the resonant absorption and emission energies due to Franck–Condon relaxations. For another sample fabricated specifically by repeated etching of the 3C-SiC wafer, the particle size is between 12 and 18 nm and constant emissions at  $\sim 550$  nm is shown.<sup>1</sup> The Stokes shift

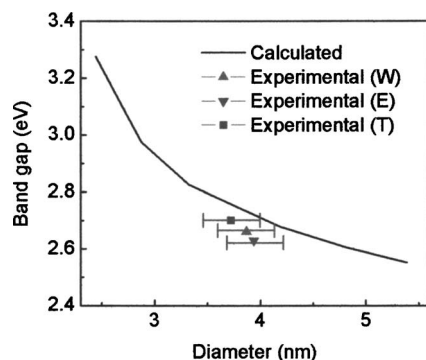


FIG. 4. (Color online) Relationship between the energy gap and diameter of 3C-SiC crystallite. The experimental data appear as solid signs with error bars representing the errors of the diameter from TEM observations. The value of the band gap corresponds to the emission wavelength at respective turning point shown in Fig. 2(a). The solid line is the theoretical result of the transition energy gap vs particle diameter of 3C-SiC quantum dot (Ref. 4).

is 0.26 eV because larger particles produce smaller Stokes shifts.

The silicon crystallites can be oxidized in seconds when exposed to air and their optical properties are altered accordingly.<sup>23</sup> In contrast, we have found that the colloidal 3C-SiC nanocrystals retain their luminescent properties after storage in air for over 3 months, although the emission does weaken slightly. Only small aggregation can be observed, and most particles remain uniformly dispersed in the solutions, demonstrating that colloidal 3C-SiC nanocrystals are very stable. The stability along with its good biocompatibility and high chemical stability<sup>24</sup> bodes well for the use of 3C-SiC nanocrystals in biological applications such as biological labeling as well as in optoelectronic applications.<sup>25,26</sup>

Our results show that the solvent in which the 3C-SiC nanocrystals are suspended plays two critical roles. First, it serves as the sustaining medium that keeps the individual 3C-SiC particles apart. Second, it provides a high potential barrier for the carriers (electrons and holes) to ensure quantum confinement. Moreover, the small influence on the luminescence demonstrates that the surrounding medium is not responsible for the difference between the as-made porous and dispersed structures. The absence of luminescence from porous 3C-SiC is possibly due to the fact that electrochemical etching leads to a structure which combines quantum-sized 3C-SiC crystallites with others that are too large to exhibit quantum confinement but are interconnected to smaller ones so that charge carriers will leak into the larger crystallites.

In summary, we have studied the effects of the solvents on the luminescent characteristics of 3C-SiC suspensions and confirmed that the PL originates from intrinsic band edge recombination of the carriers in the 3C-SiC crystallites. Our

results suggest that the crystallites having sizes smaller than  $\sim 8$  nm and good surface passivation are necessary for quantum confinement.

This work was supported by the Grant Nos. 10225416, 60476038, and 60421003 from the Natural Science Foundations of China, the LPEMST, and the special funds for Major state Basic Research Project (No. G2001CB3095) of China. Partial support was also provided by City University of Hong Kong Direct Allocation Grant No. 9360110 and Hong Kong Research Grants Council (RGC) Competitive Earmarked Research Grant No. CityU 1120/04E.

- <sup>1</sup>X. L. Wu, J. Y. Fan, T. Qiu, X. Yang, G. G. Siu, and P. K. Chu, *Phys. Rev. Lett.* **94**, 026102 (2005).
- <sup>2</sup>A. L. Efros and A. L. Efros, *Sov. Phys. Semicond.* **16**, 772 (1982).
- <sup>3</sup>L. Brus, *J. Chem. Phys.* **79**, 5566 (1983).
- <sup>4</sup>D. H. Feng, Z. Z. Xu, T. Q. Jia, X. X. Li, and S. Q. Gong, *Phys. Rev. B* **68**, 035334 (2003).
- <sup>5</sup>F. A. Reboredo, L. Pizzagalli, and G. Galli, *Nano Lett.* **4**, 801 (2004).
- <sup>6</sup>T. Matsumoto, J. Takahashi, T. Tamaki, T. Futagi, H. Mimura, and Y. Kanemitsu, *Appl. Phys. Lett.* **64**, 226 (1994).
- <sup>7</sup>J. S. Shor, L. Bemis, A. D. Kurtz, I. Grimberg, B. Z. Weiss, M. F. MacMillian, and W. J. Choyke, *J. Appl. Phys.* **76**, 4045 (1994).
- <sup>8</sup>A. O. Konstantinov, A. Henry, C. I. Harris, and E. Janzén, *Appl. Phys. Lett.* **66**, 2250 (1995).
- <sup>9</sup>V. Petrova-Koch, O. Sreseli, G. Polisski, D. Kovalev, T. Muschik, and F. Koch, *Thin Solid Films* **255**, 107 (1995).
- <sup>10</sup>L. S. Liao, X. M. Bao, Z. F. Yang, and N. B. Min, *Appl. Phys. Lett.* **66**, 2382 (1995).
- <sup>11</sup>X. L. Wu, G. G. Siu, M. J. Stokes, D. L. Fan, Y. Gu, and X. M. Bao, *Appl. Phys. Lett.* **77**, 1292 (2000).
- <sup>12</sup>Y. P. Guo, J. C. Zheng, A. T. S. Wee, C. H. A. Huan, K. Li, J. S. Pan, Z. C. Feng, and S. J. Chua, *Chem. Phys. Lett.* **339**, 319 (2001).
- <sup>13</sup>A. Kassiba, M. Makowsak-JJanusik, J. Bouclé, J. F. Bardeau, A. Bulou, and N. Herlin-Boime, *Phys. Rev. B* **66**, 155317 (2002).
- <sup>14</sup>T. L. Rittenhouse, P. W. Bohn, T. K. Hossain, I. Adesida, J. Lindesay, and A. Marcus, *J. Appl. Phys.* **95**, 490 (2004).
- <sup>15</sup>L. T. Canham, *Appl. Phys. Lett.* **57**, 1046 (1990).
- <sup>16</sup>M. D. Mason, G. M. Credo, K. D. Weston, and S. K. Buratto, *Phys. Rev. Lett.* **80**, 5405 (1998).
- <sup>17</sup>J. Y. Fan, X. L. Wu, F. Kong, T. Qiu, and G. S. Huang, *Appl. Phys. Lett.* **86**, 171903 (2005).
- <sup>18</sup>J. Heinrich, C. L. Curtis, G. M. Credo, K. L. Kavanagh, and M. J. Sailor, *Science* **255**, 66 (1992).
- <sup>19</sup>O. Akcakir, J. Therrien, G. Belomoin, N. Barry, J. D. Muller, E. Gratton, and M. Nayfeh, *Appl. Phys. Lett.* **76**, 1857 (2000).
- <sup>20</sup>Joint Committee on Powder Diffraction Standards (JCPDS) File No. 29-1129, International Center for Diffraction Data, 1982.
- <sup>21</sup>U. Woggon, *Optical Properties of Semiconductor Quantum Dots* (Springer, Berlin, 1997).
- <sup>22</sup>O. Madelung, *Semiconductors: Data Handbook*, 3rd ed. (Springer, Berlin, 2004), p. 61.
- <sup>23</sup>M. V. Wolkin, J. Jorne, P. M. Fauchet, G. Allan, and C. Delerue, *Phys. Rev. Lett.* **82**, 197 (1999).
- <sup>24</sup>H. Morkoc, S. Strite, G. B. Gao, M. E. Lin, B. Sverdlov, and M. Burns, *J. Appl. Phys.* **76**, 1363 (1994).
- <sup>25</sup>P. Moriarty, *Rep. Prog. Phys.* **64**, 297 (2001).
- <sup>26</sup>D. Kovalev, H. Heckler, G. Polisski, and F. Koch, *Phys. Status Solidi B* **215**, 871 (1999).